ISSN 0021-3640, JETP Letters, 2025, Vol. 122, No. 7, pp. 424–429. © The Author(s), 2025. This article is an open access publication.
Russian Text © The Author(s), 2025, published in Pis'ma v Zhurnal Eksperimental'noi i Teoreticheskoi Fiziki, 2025, Vol. 122, No. 7, pp. 410–415.

CONDENSED MATTER

Two-Magnon Raman Scattering in Strontium Orthoferrites

S. V. Zaitsev[a],*, V. D. Sedykh[a], and K. P. Meletov[a]

[a] *Osipyan Institute of Solid State Physics, Russian Academy of Sciences, Chernogolovka, Moscow region, 142432 Russia*

**e-mail: szaitsev@issp.ac.ru*

Received July 14, 2025; revised August 18, 2025; accepted August 26, 2025

Raman spectra have been measured in polycrystalline samples of $La_{0.5}Sr_{0.5}FeO_{3-\delta}$ and $SrFeO_{2.5}$ antiferromagnetic orthoferrites in the orthorhombic and brownmillerite phases, respectively, in the temperature range of 300–700 K. A significant decrease in the intensity of the 1300–1400 cm^{-1} band when approaching the Néel temperature ($T_N \sim 410$ K in the substituted orthoferrite $La_{0.5}Sr_{0.5}FeO_{3-\delta}$ and $T_N \sim 670$ K in the brownmillerite $SrFeO_{2.5}$) indicates magnetic ordering in the crystals under normal conditions, and the band itself is due to two-magnon scattering, in contrast to the ~1100-cm^{-1} biphonon scattering band, which retains its intensity over the entire temperature range.

DOI: 10.1134/S0021364025608565

INTRODUCTION

Perovskite oxides $R_{1-x}A_xBO_{3-\gamma}$ (R is a rare earth element; A = Ba, Ca, or Sr; and B = Fe, Mn, Co, or Ni) are promising materials due to their unusual electrical, magnetic, and catalytic properties [1, 2]. In such compounds, transition metal ions have mixed valence states, which are responsible for a high electronic conductivity at room temperature. These states can result in significant oxygen non-stoichiometry, which is due to the strong diffusion of oxygen ions. Mixed valence can be caused either by the substitution of bivalent ions (A) for the sites of the trivalent element (R) or by the formation of oxygen vacancies [3]. The magnetic properties of these complexes are due to the superexchange mechanism involving the 3*d* electrons of transition metal ions and the *p* orbitals of oxygen [4]. Thus, oxygen plays a very important role in the magnetic ordering of these compounds. The oxides in this family with the composition RBO_3 have perovskite-like crystal structures. Compounds in which the metal ion (B) is Fe are called orthoferrites and their perovskite structure is orthorhombically distorted due to the displacement of oxygen ions and rare-earth elements from sites corresponding to the cubic structure [5, 6]. $LaFeO_3$ is a multiferroic material due to the presence of bound magnetic and ferroelectric orders in it [7] and therefore can have a variety of applications, including as electrode materials for fuel cells, catalysts, chemical sensors, optoelectronic devices, magnetic memory devices, etc. [8–12]. The compound has an orthorhombic structure with the space group *Pbmn*. Iron ions in it are in a trivalent state Fe^{3+} and have an octahedral oxygen environment, and the O^{2-} anions between the 7octahedra create a superexchange interaction between Fe^{3+} ions. According to the theory, the superexchange interaction between two Fe^{3+} cations is antiferromagnetic (AFM), and stronger than that between Fe^{4+} and Fe^{3+} ions or between two Fe^{4+} cations [4]. Due to the slight deviation of the spins from the strict antiparallel orientation resulting from the zigzag arrangement of the oxygen octahedra, the samples exhibit non-collinear antiferromagnetism (weak ferromagnetism), with the superexchange interaction between Fe^{3+} ions increasing with the angle θ of a $Fe^{3+}–O^{2-}–Fe^{3+}$ bond [6]. $LaFeO_3$ has the largest bond angle in the orthoferrite family, resulting in the highest Néel temperature $T_N \approx 750$ K [7]. The partial substitution of bivalent Sr for trivalent La leads to an increase in the valence state of iron ions from Fe^{3+} to Fe^{4+}, resulting in the appearance of holes and a significant decrease in the resistivity at room temperature. Another consequence of ionic substitution of Sr^{2+} for La^{3+} in $La_{1-x}Sr_xFeO_{3-\delta}$ is the weakening of the AFM order: T_N decreases significantly with an increase in the Sr content [5].

For the study of the spectrum of magnetic excitations in magnetically ordered systems, the most informative methods are inelastic neutron scattering and optical Raman spectroscopy [13, 14]. For example, the parameters characterizing the magnetic interaction in AFM crystals with a simple magnetic structure of rutile or perovskite can be accurately determined by the Raman scattering method, similar to the neutron scattering technique [14]. The ideal cubic symmetry in most of the perovskites is broken, which

is accompanied by the appearance of longitudinal optical (LO) phonons active in the Raman spectra [15, 16]. The strong coupling of the electron system to phonon lattice oscillations in perovskites leads to the extreme sensitivity of LO phonons to oxygen content and a significant temperature dependence of their energy [17, 18]. The classification of phonon modes in the region below 1000 cm^{-1} was studied in numerous works and is quite well defined [15, 19]. For example, modes below 200 cm^{-1} in $LaFeO_3$ are referred to lattice oscillations of heavy lanthanum, modes in the range of 200–450 cm^{-1} are attributed to oscillations of lighter oxygen in inclined FeO_6 octahedra, and a strong ~650 cm^{-1} mode is referred to the in-phase stretching of Fe–O bonds [15]. At the same time, such certainty in the interpretation of modes with frequencies above 1000 cm^{-1} in orthoferrites is still absent. Due to the high energy of these modes, some authors attribute them to two-magnon scattering [16, 20], but other authors treat them as two-phonon combinations of LO phonons [6, 21]. In this regard, many authors emphasize that only studies in a wide temperature range below and above the Néel temperature can clarify the situation, as done in [20, 22]. It is interesting and important to study the temperature dependence of Raman spectra in multiferroic $BiFeO_3$ [23], where intense biphonon scattering lines sensitive to the AFM transition were observed in the Raman spectra. Furthermore, one of these lines almost disappeared above the Néel temperature $T_N \approx 375$°C, which was explained by the strong coupling between the phonon and spin systems in this compound [23]. The authors of [21] studied in detail $LaFeO_3$ modes in the energy range up to 3000 cm^{-1} in a wide temperature range below and above the Néel temperature $T_N = 740$ K. A significant decrease in the intensity of the characteristic ~1300 cm^{-1} band, as well as other bands of the spectrum, was observed when heated to T_N and above, up to the maximum temperature of 873 K, the saturation or complete disappearance of the band was not observed. In our opinion, the authors of [21] made an erroneous conclusion about the absence of correlation between this band, which is characteristic of many magnetically ordered orthoferrites, and two-magnon scattering. The fact is that two-magnon scattering in AFM perovskites can be observed not only up to the Néel temperature $T_N \sim 410$ K, but also above it due to correlations of magnetic moments, and the intensity in the AFM compound with a rutile structure initially increases even above T_N, while the frequency of the maximum of the two-magnon scattering band in all cases decreases monotonically [14].

In this work, polycrystalline samples of AFM orthoferrites $La_{0.5}Sr_{0.5}FeO_{3-\delta}$ (orthorhombic phase) and $SrFeO_{2.5}$ (brownmillerite phase) are studied by the method of Raman spectroscopy in the wide range 300–700 K from room temperature to the Néel temperature and above. With an increase in the temperature, a significant drop in the intensity of the characteristic ~1350–1400 cm^{-1} band is observed in both compounds when approaching T_N, which indicates the presence of ordering in the AFM samples, and the band itself is due to two-magnon scattering, in contrast to the bands of single- and two-phonon scattering, which retain the intensity over the entire temperature range.

SAMPLES AND THE EXPERIMENTAL METHOD

Polycrystalline $La_{1-x}Sr_xFeO_{3-\delta}$ ($x = 0$, 0.5, 1.0) samples were synthesized by the sol–gel method from Sr, Fe, and La nitrates in a stoichiometric ratio as initial reagents. Details of sample preparation, their composition, and structure are described in [24, 25]. Each sample was a conglomerate of melted particles ranging in size from fractions to tens of microns. Heat treatment insignificantly affects the size and shape of particles. Note that each member of the $La_{1-x}Sr_xFeO_{3-\delta}$ strontium orthoferrite family is a compound with an anion-deficient structure of the perovskite type (the symbol δ characterizes the content of oxygen vacancies), and Fe cations can have a mixed valence state (Fe^{3+} or Fe^{4+}). The physical properties of these oxides are extremely sensitive to the oxygen content, which depends significantly on the conditions of synthesis and heat treatment. In particular, lanthanum orthoferrite $LaFeO_3$ has complete stoichiometry in oxygen content and thereby cannot have oxygen vacancies, which is confirmed by Mössbauer spectroscopy. X-ray diffraction analysis indicates the initial orthorhombic phase *Pbnm* of the synthesized samples [24]. After synthesis, the $La_{0.5}Sr_{0.5}FeO_{3-\delta}$ sample was annealed in vacuum (10^{-3} Torr) at a temperature of $T = 650$°C for 6 h to reduce the oxygen content and create oxygen vacancies in the immediate vicinity of iron ions, converting them to the trivalent Fe^{3+} state. Previously, it was found that a significant fraction of Fe^{4+} ions in unannealed samples leads to complete suppression of phonon modes [25]. It should be noted that the Mössbauer spectroscopy data [26] indicate that the oxygen content in this annealed sample is 2.76 ± 0.05, which requires additional confirmation. After synthesis, an $SrFeO_{3-\delta}$ strontium orthoferrite sample was annealed either in a vacuum at 650°C for 10 h or in an oxygen atmosphere at 360°C for 240 h. The $SrFeO_{2.5}$ sample in the brownmillerite phase (orthorhombic phase with the group *Ibm*2) was obtained in the first case, and the $SrFeO_{2.9}$ strontium orthoferrite sample in the tetragonal phase was formed in the second case, which, after annealing in oxygen, has a composition close to complete stoichiometry in oxygen content of 2.93 ± 0.03, which was established by X-ray spectral analysis [24].

Raman spectra were measured in backscattering geometry on a facility equipped with a homemade

optical thermostat designed for Raman measurements in microsamples from room temperature to ~750 K. The stabilization system ensures maintaining the temperature within ±4°C. The optical part of the facility includes an Acton SpectraPro-2500i spectrograph with a CCD detector Pixis2K cooled to –70°C and an Olympus BX51 microscope. To excite Raman scattering, we used a solid-state single-mode cw laser with a wavelength of $\lambda = 532$ nm. The laser beam was focused on the sample with a 50× Olympus SLMPLN objective with a numerical aperture of 0.35, and a working distance of 18 mm. the laser radiation line in the scattered beam was suppressed by an edge filter for $\lambda = 532$ nm with an optical density of $OD = 6$ and a passband shift of ~60 cm^{-1}, and the intensity of the laser excitation immediately in front of the sample was ~1 mW.

RESULTS AND THEIR DISCUSSION

Figure 1 shows the Raman spectra of $LaFeO_3$ lanthanum orthoferrite, $La_{0.5}Sr_{0.5}FeO_{3-\delta}$ substituted lanthanum orthoferrite, and $SrFeO_{2.93}$ strontium orthoferrite at room temperature. It can be seen that the $SrFeO_{2.93}$ sample obtained by annealing in an oxygen atmosphere and having an oxygen stoichiometry close to the ideal for perovskites (3.0) has very weakly expressed LO phonons in the Raman spectrum (marked with arrows in Fig. 1), which is due to a weak violation of cubic symmetry (tetragonal phase). The matter is that an ideal ABO_3 perovskite of cubic symmetry with La ions in the lattice nodes A and Fe ions in the center of oxygen octahedra B should not have Raman-active phonon modes for symmetry reasons [6]. However, in most of the real perovskites, symmetry is broken due to the displacement of ions from the positions of the ideal cubic structure, which leads to the appearance of LO phonons in the Raman spectra. In particular, as shown in [17], the sequential annealing of a thin $La_{0.2}Sr_{0.8}FeO_3$ film leads not only to the loss of oxygen with a simultaneous increase in the resistance, but also to a change in the crystal structure from rhombohedral to brownmillerite structure, which results in the activation of modes in the range of 400–800 cm^{-1} in the Raman spectrum. In $LaFeO_3$ lanthanum orthoferrite, which is crystallized in the orthorhombic phase, LO phonons are initially pronounced (see Fig. 1). Similarly, in the $La_{0.5}Sr_{0.5}FeO_{3-\delta}$ substituted orthoferrite, which also has a orthorhombic structure, less intense LO phonons are clearly pronounced, but strongly broadened and blueshifted (see Fig. 1). A significant broadening of all Raman lines in $La_{0.5}Sr_{0.5}FeO_{3-\delta}$ is naturally attributed to the local disorder, which occurs when strontium is substituted for lanthanum. The strong microscopic inhomogeneity of the charge state of Fe^{4+}/Fe^{3+} ions and the associated oxygen vacancies arising during vacuum annealing additionally contributes to disorder. The inset of Fig. 1

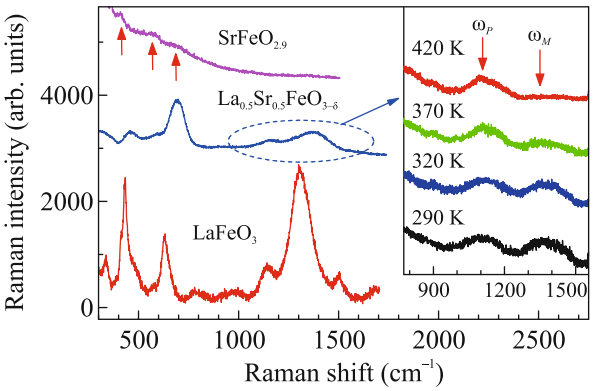

Fig. 1. (Color online) Raman spectra of samples at room temperature (sequentially shifted up vertically): $LaFeO_3$ lanthanum orthoferrite (orthorhombic phase), substituted $La_{0.5}Sr_{0.5}FeO_{3-\delta}$ orthoferrite after vacuum annealing (orthorhombic phase), and $SrFeO_{2.9}$ strontium orthoferrite after annealing in oxygen (tetragonal phase). The inset shows the spectra of the $La_{0.5}Sr_{0.5}FeO_{3-\delta}$ sample above 800 cm^{-1} at different temperatures.

shows the Raman spectra above 800 cm^{-1} from room temperature to the Néel temperature, which was estimated after vacuum annealing from the temperature dependence of the magnetic moment $M(T)$ at $T_N \approx 410$ K [26]. The Raman spectrum in this spectral range has two pronounced bands $\omega_P \sim 1120$ and ~ 1370 cm^{-1}. As can be seen in Fig. 1, the intensity of the ω_M band decreases monotonically to almost zero between 370 and 420 K, i.e., above T_N, while the ω_P band changes slightly. The experimentally observed strong decrease in the band intensity to the background level near the Néel temperature T_N is similar to the behavior of two-magnon scattering in previously studied AFM perovskites [14]. At the same time, the weak temperature dependence of the band corresponds to the behavior of biphonon scattering, and the band itself is probably associated with the combination of the two strongest phonons at ~465 and ~695 cm^{-1} in this sample (see Fig. 1).

The low intensity of bands above 1000 cm^{-1} significantly complicates the processing of the temperature dependence of Raman spectra in substituted orthoferrite samples. For this reason, for a more detailed study of the two-magnon scattering in this system, the $SrFeO_{2.5}$ brownmillerite phase ($Sr_2Fe_2O_5$ in another designation) was chosen with a higher intensity of Raman spectra above 1000 cm^{-1} at room temperature [27] and having a higher Néel temperature $T_N \approx 670$ K [28]. The Raman spectra of this sample from room temperature to T_N and above are shown in Fig. 2 together with the spectrum of the sample cooled to room temperature after the end of the temperature series (marked as 294 K after), which is almost the same as the original spectrum (specified as 294 K

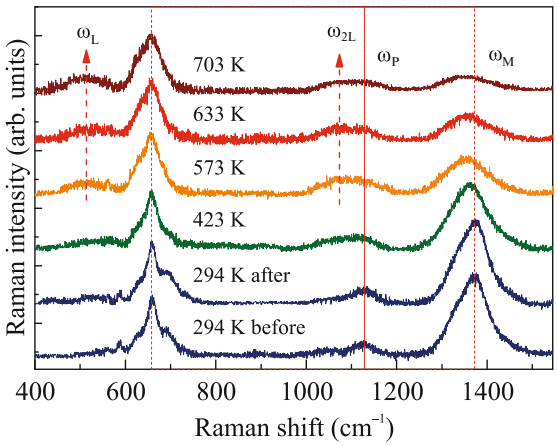

Fig. 2. (Color online) Spectra of the $SrFeO_{2.5}$ brownmillerite phase sample normalized to the ~660 cm^{-1} phonon mode and sequentially shifted vertically. For convenient processing, the nonlinear background is subtracted from the spectra. For comparison, the spectra of the original sample (294 K before) and after the end of the temperature series (294 K after) are given.

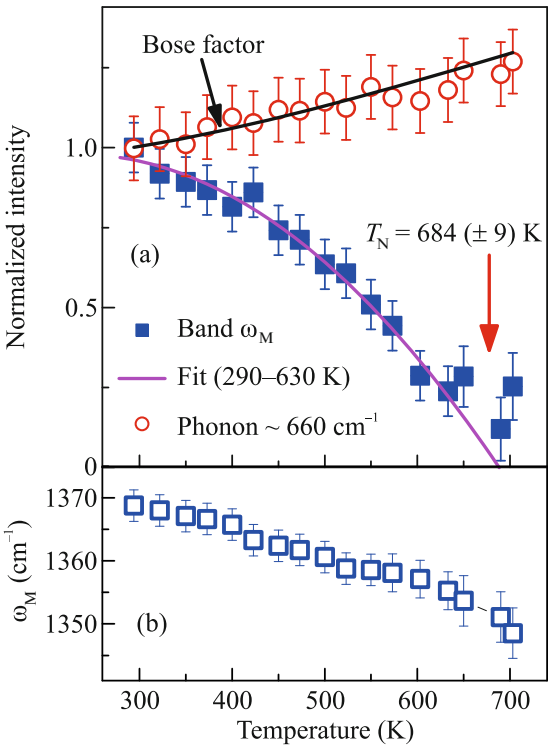

Fig. 3. (Color online) (a) (Squares) Temperature dependence of the relative intensity of the band ω_M in the $SrFeO_{2.5}$ sample, (violate solid line) its second-order polynomial approximation in the interval $T = 294–630$ K, (circles) the integral intensity of the ~660 cm^{-1} phonon mode together with its ~630 cm^{-1} and ~690 cm^{-1} satellites, and (black line) the temperature factor $S(\omega,T)$ for Stokes components of phonon modes (see the main text). All data are normalized to the values at $T = 294$ K. (b) Temperature dependence of the frequency of the band maximum ω_M.

before) and shows the stability of the samples during thermal cycling during the measurement process. It can be seen that a strong mode at ~660 cm^{-1} is pronounced in the low-frequency region, which corresponds to the in-phase stretching of Fe–O bonds in FeO_6 octahedra [15]. This band has two pronounced shoulders at ~630 and ~690 cm^{-1}, which can be attributed to different local oxygen environments of Fe^{3+} ions, which is characteristic of the $SrFeO_{2.5}$ brownmillerite phase [24]. With an increase in temperature, the ~660 cm^{-1} mode is broadened noticeably, but its absolute intensity at the peak changes slightly, and the maximum of the band itself is hardly shifted (see Fig. 2). Figure 3a shows the temperature dependence of the integral relative intensity of this phonon mode together with its satellites (shoulders ~630 and ~690 cm^{-1}), normalized to the value at $T =$ 294 K, and the black solid line also shows the normalized dependence of the temperature multiplier $S(\omega, T)$ for the Stokes components of the phonon modes (Bose factor), which is related to the Bose–Einstein distribution $n(\hbar\omega, kT)$) as:

$$S(\omega,T) = 1 + n(\hbar\omega/kT) = 1 + 1/\{\exp(\hbar\omega/kT) - 1\}, \quad (1)$$

where $\hbar\omega$ is the energy of the mode (Raman shift) [14]. Good agreement of the Bose factor $S(\omega, T)$ with the experimental dependence of the intensity of this phonon mode is seen.

The high-energy part of the Raman spectra demonstrates a different behavior. With an increase in the temperature, the intensity of the characteristic band (~1370 cm^{-1} at 300 K) drops significantly and its maximum is redshifted. However, the ω_M band does not disappear completely at high temperatures, unlike that in the $La_{0.5}Sr_{0.5}FeO_{3-\delta}$ substituted orthoferrite (see Fig. 1). Similarly, the ω_P band (~1130 cm^{-1} at 300 K) behaves in a more complex way: it has a wide satellite ω_{2L} at ~1075 cm^{-1} above ~400 K, while both lines are maintained up to 700 K, slightly changing in intensity (see Fig. 2). Interestingly, simultaneously with the ω_{2L} satellite, the ω_L band appears in the low-frequency region of ~490–550 cm^{-1} (see Fig. 2). The origin of the ω_L and ω_{2L} bands is currently unclear and requires further investigation. The stability of the ω_P band with temperature also indicates a biphonon origin, apparently as a combination of the strongest ~660 cm^{-1} phonon mode and some other, but an unambiguous answer requires a study at high pressures, which will also allow us to identify a possible biphonon contribution in the ω_M band region. However, a significant decrease in the intensity near the

Néel temperature is observed only in the ω_M band. Figure 3a shows the temperature dependence of the relative intensity of the ω_M band normalized to its value at room temperature, and the solid line shows the second-order polynomial approximation of this dependence in the range $T = 290–630$ K. The point of intersection of the approximation curve with the x axis at 684 ± 9 K agrees well with the Néel temperature $T_N \approx 673$ K of the $SrFeO_{2.5}$ brownmillerite phase, which was determined from the temperature dependence of the magnetic susceptibility [28]. The maximum of the ω_M band is redshifted with an increase in the temperature (see Fig. 3b), in contrast to the ω_P biphonon scattering band. The band itself is clearly pronounced and has a noticeable intensity $I(700\text{ K}) \sim 0.15I(300\text{ K})$ above the Néel temperature T_N (see Fig. 3a), which indicates a significant role of AFM fluctuations above T_N, in accordance with the theory (see [14] and references therein). The observed behavior is fully consistent with the temperature behavior of the two-magnon scattering band previously observed in AFM perovskites, which gives us reason to attribute the ω_N band to two-magnon scattering.

CONCLUSIONS

In this work, polycrystalline samples of $La_{0.5}Sr_{0.5}FeO_{3-\delta}$ antiferromagnetic orthoferrites (orthorhombic phase) and $SrFeO_{2.5}$ (brownmillerite phase) have been studied by the Raman method in the wide temperature range of 300–700 K. A significant decrease in the intensity and a noticeable redshift (in $SrFeO_{2.5}$) of the characteristic high-energy ~1300–1400 cm^{-1} band has been observed when approaching the Néel temperature T_N, which makes it possible to attribute it to two-magnon scattering in magnetically ordered samples, in contrast to the ~1100 cm^{-1} biphonon scattering band, which retains its intensity and position over the entire temperature range.

FUNDING

This work was supported by the Ministry of Science and Higher Education of the Russian Federation (state assignment of the Osipyan Institute of Solid State Physics, Russian Academy of Sciences).

CONFLICT OF INTEREST

The authors of this work declares that they have no conflicts of interest.

OPEN ACCESS

REFERENCES

1. M. B. Salamon and M. Jaime, Rev. Mod. Phys. **73**, 583 (2001).
2. Y. Tokura, *Contribution to Colossal Magnetoresistance Oxides,* Ed. by Y. Tokura (Gordon and Breach, London, 1999).
3. J. B. Yang, W. B. Yelon, W. J. James, Z. Chu, M. Kornecki, Y. X. Xie, X. D. Zhou, H. U. Anderson, A. G. Joshi, and S. K. Malik, Phys. Rev. B **66**, 184415 (2002).
4. J. B. Goodenough, in *Magnetism and Chemical Bond,* Ed. by F. A. Cotton (Interscience, London, 1963), Vol. 1.
5. R. B. da Silva, J. M. Soares, J. A. P. da Costa, J. H. de Araujo, A. R. Rodrigues, and F. L. A. Machado, J. Magn. Magn. Mater. **466**, 306 (2018).
6. S. Manzoor and S. Husain, J. Appl. Phys. **124**, 065110 (2018).
7. S. Phokha, S. Pinitsoontorn, S. Rujirawat, and S. Maensiri, Phys. B (Amsterdam, Neth.) **476**, 55 (2015).
8. E. A. Tugova, V. F. Popova, I. A. Zvereva, and V. V. Gusarov, Glass Phys. Chem. **32**, 674 (2006).
9. S. Petrovic, A. Terlecki-Baricevic, L. Karanovic, P. Kirilov-Stefanov, M. Zdujic, V. Dondur, D. Paneva, I. Mitov, and V. Rakic, Appl. Catal. B: Environ. **79**, 186 (2008).
10. S. N. Tijare, M. V. Joshi, P. S. Padole, P. A. Mangrulkar, S. Rayalu, and N. K. Labhsetwar, Int. J. Hydrogen Energy **37**, 10451 (2012).
11. Z. Wei, Y. Xu, H. Liu, and C. Hu, J. Hazard. Mater. **165**, 1056 (2009).
12. J. Faye, A. Bayleta, M. Trentesaux, S. Royera, F. Dumeignil, D. Duprez, and S. Valange, Appl. Catal., B **126**, 134 (2012).
13. W. Lehmann and R. Weber, J. Phys. C: Solid State Phys. **10**, 97 (1977).
14. M. G. Cottam and D. J. Lockwood, *Light Scattering in Magnetic Solids* (Wiley, New York, 1986).
15. M. C. Weber, M. Guennou, H. J. Zhao, J. Iniguez, R. Vilarinho, A. Almeida, J. A. Moreira, and J. Kreisel, Phys. Rev. B **94**, 214103 (2016).
16. J. Andreasson, J. Holmlund, C. S. Knee, M. Kall, L. Borjesson, S. Naler, J. Backstrom, M. Rubhausen, A. K. Azad, and S.-G. Eriksson, Phys. Rev. B **75**, 104302 (2007).
17. M. A. Islam, Y. Xie, M. D. Scafetta, S. J. May, and J. E. Spanier, J. Phys.: Condens. Matter **27**, 155401 (2015).

18. Sh. Ghosh, N. Kamaraju, M. Seto, A. Fujimori, Y. Takeda, S. Ishiwata, S. Kawasaki, M. Azuma, M. Takano, and A. K. Sood, Phys. Rev. B **71**, 245110 (2005).
19. M. N. Iliev, M. V. Abrashev, J. Laverdiere, S. Jandl, M. M. Gospodinov, Y.-Q. Wang, and Y.-Y. Sun, Phys. Rev. B **73**, 064302 (2006).
20. S. Manzoor, S. Husain, and V. Raghavendra Reddy, Appl. Phys. Lett. **113**, 072901 (2018).
21. J. Andreasson, J. Holmlund, R. Rauer, M. Kall, L. Borjesson, C. S. Knee, A. K. Eriksson, S. G. Eriksson, M. Rubhausen, and R. P. Chaudhury, Phys. Rev. B **78**, 235103 (2008).
22. M. J. Massey, U. Baier, R. Merlin, and W. H. Weber, Phys. Rev. B **41**, 7822 (1990).
23. M. O. Ramirez, M. Krishnamurthi, S. Denev, A. Kumar, S.-Y. Yang, Y.-H. Chu, E. Saiz, J. Seidel, A. P. Pyatakov, A. Bush, D. Viehland, J. Orenstein, R. Ramesh, and V. Gopalan, Appl. Phys. Lett. **92**, 022511 (2008).
24. V. D. Sedykh, O. G. Rybchenko, A. N. Nekrasov, I. E. Koneva, and V. I. Kulakov, Phys. Solid State **61**, 1099 (2019).
25. A. I. Dmitriev, S. V. Zaitsev, M. S. Dmitrieva, O. G. Rybchenko, and V. D. Sedykh, Fiz. Tverd. Tela **66**, 386 (2024).
26. V. D. Sedykh, O. G. Rybchenko, V. S. Rusakov, A. M. Gapochka, A. I. Dmitriev, E. A. Pershina, S. V. Zaitsev, K. P. Meletov, V. I. Kulakov, and A. I. Ivanov, Fiz. Tverd. Tela **67**, 206 (2025).
27. A. I. Dmitriev, S. V. Zaitsev, and M. S. Dmitrieva, Fiz. Tverd. Tela **67**, 156 (2025).
28. M. Schmidt and S. J. Campbell, J. Solid State Chem. **156**, 292 (2001).

Translated by R. Tyapaev